

Two Bounds on the Maximum Phonon-Mediated Superconducting Transition Temperature

Jonathan E. Moussa* and Marvin L. Cohen

*Department of Physics, University of California at Berkeley, and Materials Sciences Division,
Lawrence Berkeley National Laboratory, Berkeley, California 94720, USA*

(Dated: August 4, 2021)

Two simple bounds on the T_c of conventional, phonon-mediated superconductors are derived within the framework of Eliashberg theory in the strong coupling regime. The first bound is set by the total electron-phonon coupling available within a material given the hypothetical ability to arbitrarily dope the material. This bound is studied by deriving a generalization of the McMillan-Hopfield parameter, $\tilde{\eta}(E)$, which measures the strength of electron-phonon coupling including anisotropy effects and rigid-band doping of the Fermi level to E . The second bound is set by the softening of phonons to instability due to strong electron-phonon coupling with electrons at the Fermi level. We apply these bounds to some covalent superconductors including MgB_2 , where T_c reaches the first bound, and boron-doped diamond, which is far from its bounds.

PACS numbers: 74.20.-z, 74.62.Dh, 74.62.Bf, 74.25.Kc

I. INTRODUCTION

With the discovery of increasingly high transition temperatures for conventional BCS superconductors, it is of interest to reassess and rederive bounds on the maximum possible T_c . The goal in this area of research is to provide useful theoretical guidelines for the continued search for higher T_c materials. In the work of Cohen and Anderson¹, three different arguments give three different bounds on T_c . The first of these arguments is simply based on the form of the McMillan T_c formula², which gives a maximum T_c proportional to a material's average phonon energy ω_{ph} for all values of the electron-phonon coupling constant λ . However, the McMillan formula is only valid in the $\lambda \lesssim 1$ regime and the correct Eliashberg T_c formula for large λ is³

$$T_c \sim \sqrt{\lambda} \omega_{ph}, \quad (1)$$

which is unbounded in λ and potentially much larger than ω_{ph} . The second argument of Cohen and Anderson postulates that stability requires the static dielectric function of a material to be positive, which leads to an upper bound on T_c of approximately 10 K. This bound and stability requirement are subsequently dismissed in the paper because of the neglect of local fields and umklapp processes, and further work⁴ has clarified that stability only requires a positive static dielectric function at long wavelengths. This second argument is refined and it is concluded that strong electron-phonon coupling is limited by an instability leading to insulating, covalently bonded materials. Strong covalent bonds and superconductivity are not mutually exclusive, most notably in the case of MgB_2 ⁵, but engineering their coexistence is a difficult materials problem. The final argument examines the structural instability resulting from phonon softening due to the same electron-phonon coupling that causes superconductivity. Within the framework of a simple semiconductor model, it is shown that a phonon can go unstable before T_c reaches a maximum, further reducing

the bound from the naive $T_c \sim \omega_{ph}$. Expressions relating phonon softening to λ have since been generalized^{6,7,8,9,10} and take the form

$$\lambda \sim \frac{\Omega_{ph}^2 - \omega_{ph}^2}{\omega_{ph}^2}, \quad (2)$$

where Ω_{ph} is a bare phonon frequency.

These previous studies are revisited here in a more general framework to attempt to obtain more rigorous upper bounds on T_c . First, the strong coupling limit of Eliashberg theory is clarified through the use of upper and lower bounds on T_c . An approximation for T_c and electron-phonon coupling are directly related to the properties of the constituent atoms and their local environments within a material. We examine this measure of electron-phonon coupling as a function of electron energy to give insight into how a material might achieve a higher T_c based on modifications of its electronic structure. We then derive a structural instability bound on T_c through the calculation of the phonon softening caused by the same phonon-mediated pairing interaction that forms Cooper pairs near the Fermi surface. These methods are applied to probing the limits of superconductivity in three boron-carbon covalent metals: MgB_2 , Li_{1-x}BC , and boron-doped diamond.

The primary result of this paper is that there are two fundamental bounds on the transition temperature of a phonon-mediated superconductor, one set by lattice stability and the other by the total strength of available electron-phonon coupling. The lattice stability T_c bound can be approximately derived just from equations (1) and (2). Through substitution, the strong coupled T_c formula can be written without λ as

$$T_c \sim \sqrt{\Omega_{ph}^2 - \omega_{ph}^2}, \quad (3)$$

which is maximized as the electron-phonon coupling grows, $\lambda \rightarrow \infty$, softening the phonon frequency towards

instability, $\omega_{ph} \rightarrow 0$. This suggests that Eliashberg theory does not have an unbounded T_c as Eq. (1) might lead us to believe, but rather it is proportional to a bare phonon frequency Ω_{ph} that can be larger than the softened phonon frequencies observed in a superconducting material. Another form that Eq. (1) is sometimes written as is

$$T_c \sim \sqrt{\frac{\eta}{M}}, \quad (4)$$

where M is an averaged atomic mass and η is the McMillan-Hopfield parameter³. The η has units of a spring constant and is related to the strength of the electronic response of electrons at the Fermi surface to perturbations of the atoms in the crystal. For a given M , a T_c bound is set by the maximum η possible considering all energies at the Fermi level accessible through chemical doping or other physical modifications of the material. A large η is required to approach the T_c bound set by phonon stability in materials with strong covalent bonds and a large Ω_{ph} . Approaching the phonon stability bound in systems containing strong covalent bonds will require careful material design.

II. ELIASHBERG T_c BOUNDS

The T_c calculated from the isotropic Eliashberg equations has been the subject of both upper and lower bound studies^{3,11}. In the isotropic case, the T_c of a material is uniquely determined by the Eliashberg spectral function $\alpha^2 F(\omega)$ that characterizes the electron-phonon coupling and the Coulomb parameter μ^* that quantifies the strength of the screened electron-electron Coulomb repulsion. Approximate formulas for T_c usually represent the average electron-phonon coupling by

$$\lambda \equiv 2 \int_0^\infty \alpha^2 F(\omega) \omega^{-1} d\omega, \quad (5)$$

and an average phonon frequency defined by a weighting function $f(\omega)$,

$$\langle f(\omega) \rangle \equiv \frac{2}{\lambda} \int_0^\infty f(\omega) \alpha^2 F(\omega) \omega^{-1} d\omega. \quad (6)$$

At large temperatures, T only appears in the Eliashberg equations as $\lambda \langle \omega^2 \rangle / T^2$, which is where the asymptotic T_c formula of Eq. (1) originates³. If only $\lambda \langle \omega^2 \rangle$ is specified, T_c cannot be precisely determined, but it can be bounded from above and below,

$$0 \leq T_c \leq 0.183 \sqrt{\lambda \langle \omega^2 \rangle}. \quad (7)$$

Both bounds can be attained by an Einstein model phonon spectrum,

$$\alpha^2 F(\omega)_E = \lambda \omega_E \delta(\omega - \omega_E) / 2, \quad (8)$$

the lower bound corresponding to $\omega_E \rightarrow \infty$ and the upper bound corresponding to $\omega_E \rightarrow 0$ ^{3,11}. The spectra associated with the two bounds are both unphysical pathologies, corresponding to the cases of maximum phonon softening and infinite phonon hardening.

We attempt to tighten the bounds by independently constraining λ and $\langle \omega^2 \rangle$ as well as specifying μ^* . It is already known³ that the Einstein spectrum maximizes T_c for a given λ and $\langle \omega^2 \rangle$. However, the lower bound on T_c is still zero even with these additional constraints. This is due to a pathological spectral function with two peaks, one approaching zero and the other diverging to infinity. In order to obtain a nontrivial lower bound, additional constraints need to be placed on the spectral function, and we choose the added restriction of a maximum phonon frequency ω_{max} that replaces the upper limit of integration in Eq. (5) and (6). The spectral function that minimizes T_c at fixed λ , $\langle \omega^2 \rangle$, and ω_{max} is numerically determined¹² to be

$$\alpha^2 F(\omega)_{min} = \frac{\lambda \omega}{2\omega_{max}^2} ((\omega_{max}^2 - \langle \omega^2 \rangle) \delta(\omega) + \langle \omega^2 \rangle \delta(\omega - \omega_{max})). \quad (9)$$

The phonon at $\omega = 0$ contributes to λ but not to T_c , making this effectively an Einstein spectrum when calculating T_c . The qualitative result here is that T_c is maximized when the spectral function has no width and it is minimized when all the spectral weight is pushed to the edges of the allowed frequency interval. The stronger, more complicated T_c bounds take the form

$$f(\lambda \langle \omega^2 \rangle / \omega_{max}^2, \mu^*) \omega_{max} \leq T_c \leq f(\lambda, \mu^*) \sqrt{\langle \omega^2 \rangle}. \quad (10)$$

The function $f(\lambda, \mu^*)$ smoothly interpolates between the $\exp(-1/\lambda)$ weak coupling limit and the $\sqrt{\lambda}$ strong coupling limit and can be empirically fit to

$$f(\lambda, \mu^*) = 0.69 \exp\left(-\frac{1+\lambda}{\lambda-\mu^*}\right) \sqrt{\frac{1+0.52\lambda}{1+5.6\mu^*}} \quad (11)$$

for $\lambda > \mu^*$, otherwise $f = 0$. This functional form is chosen to balance simplicity and accuracy and to match exact analytic results¹³ for $0 \leq \lambda < 0.4$ and $\lambda \gg 1$. The coefficients were chosen based on a least squares fit on the interval $0.4 \leq \lambda \leq 20$ and $0 \leq \mu^* \leq 0.2$. The average root-mean-squared deviation of f is 0.01 and the max deviation is 0.03.

We plot the upper and lower bounds of T_c for a reasonable but arbitrary $\omega_{max} = 1.5 \sqrt{\langle \omega^2 \rangle}$ as well as the McMillan formula for an Einstein spectrum in figure 1. The McMillan formula deviates perceptibly from the upper bound around $\lambda = 0.5$, by $\lambda = 1$ the deviation is roughly 20%, and after $\lambda = 2$ it passes below the lower bound chosen for the figure. The relative width of the T_c bound, $(T_c^{max} - T_c^{min}) / T_c^{max}$, is largest at weak coupling. It has been observed that T_c is more accurately proportional to a logarithmically averaged phonon frequency,

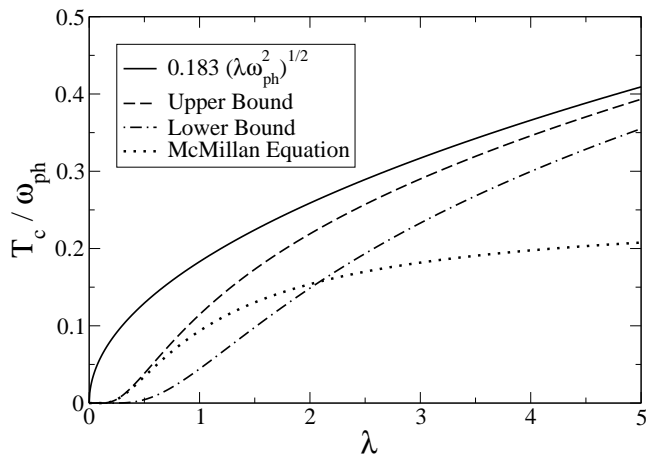


FIG. 1: Comparison of T_c upper and lower bounds (assuming $\omega_{max} = 1.5\sqrt{\langle\omega^2\rangle}$) with the McMillan formula for an Einstein spectrum of frequency ω_{ph} with a varying electron-phonon coupling strength λ and $\mu^* = 0$.

$\exp(\langle\ln(\omega)\rangle)$, rather than ω_{max} or $\sqrt{\langle\omega^2\rangle}$ in the weak-coupling regime³. As a result of that analysis, the most widely used formula for calculating T_c is the McMillan formula modified to include a log-averaged phonon frequency. In the strong coupling regime that is of more interest here, $\lambda \gtrsim 1$, both upper and lower bounds on T_c are proportional to $\sqrt{\lambda\langle\omega^2\rangle}$ and converge as λ grows.

To complete our discussion of T_c bounds, we need to address the effects of anisotropy. The anisotropy of the Eliashberg spectral function causes an increase in T_c from that calculated in the isotropic approximation¹⁴. The reason for this enhancement is an increase in λ due to anisotropy, most notably essential for describing the superconductivity in MgB₂^{15,16}, raising λ from 0.77 to 1.01. The simplest model in which to consider this effect is a multiband superconductor, which introduces a band index to the Eliashberg equations¹⁷. There is a separate gap value for each band i , $\Delta_i(\omega)$, and λ and $\lambda\langle\omega^2\rangle$ are separated into phonon processes that couple band i to band j ,

$$\lambda_{ij} \equiv 2 \int_0^\infty \alpha^2 F_{ij}(\omega) \omega^{-1} d\omega \quad (12)$$

and

$$[\lambda\langle\omega^2\rangle]_{ij} \equiv 2 \int_0^\infty \alpha^2 F_{ij}(\omega) \omega d\omega. \quad (13)$$

As in the isotropic case, for high temperatures the Eliashberg equations only contain T in terms of the form $[\lambda\langle\omega^2\rangle]_{ij}/T^2$. Correspondingly, the simple bounds on T_c are the same as Eq. (7) with $\lambda\langle\omega^2\rangle$ replaced by the largest eigenvalue of $[\lambda\langle\omega^2\rangle]_{ij}$. Both λ_{ij} and $[\lambda\langle\omega^2\rangle]_{ij}$ can be related back to the isotropic approximation by

$$\square = \sum_{ij} \frac{N_i(E_F)}{N(E_F)} \square_{ij}, \quad (14)$$

where \square is λ or $\lambda\langle\omega^2\rangle$, $N_i(E_F)$ is the density of states in the i^{th} band at the Fermi level, and $N(E_F) = \sum_i N_i(E_F)$ is the total density of states at the Fermi level. The largest eigenvalue of \square_{ij} can be written variationally as

$$\max_{x_i} \frac{\sum_{ij} x_i x_j N_i(E_F) \square_{ij}}{\sum_i x_i^2 N_i(E_F)}. \quad (15)$$

The isotropic value corresponds to $x_i = 1$, less than or equal to the maximum value. Starting from the isotropic lower bound spectral function in Eq. (9), any anisotropic perturbations at fixed λ , $\langle\omega^2\rangle$, and ω_{max} can only increase the largest eigenvalues of λ_{ij} and $[\lambda\langle\omega^2\rangle]_{ij}$ and thus only increase T_c . The lower bound of Eq. (10) cannot be lowered by anisotropy and still applies in the anisotropic case. For simple calculations of T_c upper bounds, we define effective electron-phonon coupling expressions that don't require detailed information about the anisotropy of a system,

$$\begin{aligned} \tilde{\lambda} &\equiv \sum_i \lambda_{ii} \\ \langle\tilde{\omega}^2\rangle &\equiv \tilde{\lambda}^{-1} \sum_i [\lambda\langle\omega^2\rangle]_{ii}. \end{aligned} \quad (16)$$

Both $\tilde{\lambda}$ and $\langle\tilde{\omega}^2\rangle$ will always be larger than the largest eigenvalues of λ_{ij} and $[\lambda\langle\omega^2\rangle]_{ij}$ respectively because they are each the trace of a positive definite matrix. In the isotropic case, $\tilde{\lambda}$ equals λ and $\langle\tilde{\omega}^2\rangle$ equals $\langle\omega^2\rangle$. Starting from the isotropic upper bound spectral function in Eq. (8), any anisotropic perturbations at fixed $\tilde{\lambda}$ and $\langle\tilde{\omega}^2\rangle$ can only redistribute the magnitude of the largest eigenvalues of λ_{ij} and $[\lambda\langle\omega^2\rangle]_{ij}$ to smaller eigenvalues and thus only decrease T_c . Another important effect of anisotropy is in reducing the effects of μ^* on T_c ¹⁸, the effective μ^* being determined by the distribution of the gap between bands,

$$\mu_{eff}^* \sim \sum_{ij} \Delta_i \mu_{ij}^* \Delta_j, \quad (17)$$

which in cases of extreme anisotropy can completely nullify the effect of μ^* . The end result is that the upper bound of Eq. (10) still applies to the anisotropic case provided that $\tilde{\lambda}$ and $\langle\tilde{\omega}^2\rangle$ replace the isotropic values and μ^* is set to zero.

The anisotropic case now provides additional difficulty in the strong coupling limit because $\lambda\langle\omega^2\rangle$ and $\tilde{\lambda}\langle\tilde{\omega}^2\rangle$ don't necessarily converge to each other and there is no unique simple measure of T_c that is independent of anisotropic details. Rather than resort to a more complicated expression, we examine the accuracy of λ and $\tilde{\lambda}$ in a common anisotropic scenario. Most conventional BCS superconductors are reasonably isotropic and one of the most anisotropic BCS superconductors known, MgB₂, fits well into a two band model^{15,16}. In this model, there is a strongly coupled σ -band Fermi sheet and a more weakly coupled π -band sheet. We take a more extreme

version of this two band case, where the second band has no electron-phonon coupling at the Fermi surface. In this case, the correct anisotropic result is $[\lambda\langle\omega^2\rangle]_{11}$, which is also equal to the upper bound $\tilde{\lambda}\langle\tilde{\omega}^2\rangle$. The isotropic approximation $\lambda\langle\omega^2\rangle$ equals $N_1(E_F)/N(E_F)[\lambda\langle\omega^2\rangle]_{11}$ and can substantially underestimate the correct result depending on how much of the density of states at the Fermi level lies in the decoupled band. In general, $\tilde{\lambda}$ will be correct for single-gap superconductors and the error for multi-gap superconductors will be proportional to the total magnitude of all gaps excluding the largest. For this reason, we consider $\tilde{\lambda}\langle\tilde{\omega}^2\rangle$ to be a better approximation than $\lambda\langle\omega^2\rangle$ for calculations of anisotropic superconductivity.

Assuming that we are able to enter the strong coupling regime, we are guaranteed to increase T_c uniformly if we focus solely on increasing $\tilde{\lambda}\langle\tilde{\omega}^2\rangle$. This approach works especially well if we consider classes of materials with similar Ω_{ph} because Eq. (2) shows that increasing $\tilde{\lambda}\langle\tilde{\omega}^2\rangle$ also increases $\tilde{\lambda}$ due to phonon softening. It can also be detrimental to independently consider $\tilde{\lambda}$ and $\langle\tilde{\omega}^2\rangle$ in classes of materials such as is portrayed in Eq. (9). Increasing the coupling to the very low frequency modes of a system most efficiently increases $\tilde{\lambda}$ but doesn't raise T_c . In such an extreme case, it is more useful to have a metric for superconductivity that is insensitive to low frequency coupling, which is true of $\tilde{\lambda}\langle\tilde{\omega}^2\rangle$. We make no attempts to model μ^* as it is typically between 0.1 and 0.15 in metals¹⁹ and variations of this magnitude can only change T_c by a few percent in the strong coupling regime. We are left with a single quantity to optimize, $\tilde{\lambda}\langle\tilde{\omega}^2\rangle$, that serves as a simple metric for enhancing T_c .

III. LOCAL APPROXIMATIONS

As was first pointed out by McMillan², the quantity $\lambda\langle\omega^2\rangle$ is independent of the details of the phonon spectrum. It can be written as a sum of atomic contributions

$$\lambda\langle\omega^2\rangle = \sum_i \frac{\eta_i}{M_i}, \quad (18)$$

where i is summed over all atoms in the unit cell, M_i are the atomic masses, and η_i are the McMillan-Hopfield parameters of the atoms. The quantity $\tilde{\lambda}\langle\tilde{\omega}^2\rangle$ is also independent of the phonon spectrum and can also be written as a sum of effective McMillan-Hopfield parameters,

$$\tilde{\lambda}\langle\tilde{\omega}^2\rangle = \sum_i \frac{\tilde{\eta}_i}{M_i}. \quad (19)$$

From the definition of $\tilde{\lambda}\langle\tilde{\omega}^2\rangle$ in Eq. (16) and McMillan's derivation of η it follows that

$$\tilde{\eta}_i = \sum_{n\mathbf{k}} \left| \langle n, \mathbf{k} | \frac{\partial V_{SCF}}{\partial \mathbf{R}_i} | n, \mathbf{k} \rangle \right|^2 \delta(E_F - E_{n\mathbf{k}}), \quad (20)$$

where $\partial V_{SCF}/\partial \mathbf{R}_i$ is the change in the self-consistent potential due to a change in the i th atomic position, and $|n, \mathbf{k}\rangle$ and $E_{n\mathbf{k}}$ are the Bloch wave function and band energy for band n and wavevector \mathbf{k} . Just as with $\tilde{\lambda}$, $\tilde{\eta}_i$ is less than or equal to $\tilde{\eta}_i$ with equality occurring in the isotropic case. We can generalize the electron-phonon coupling parameter $\tilde{\eta}_i$ to electrons away from the Fermi surface, at an energy E , simply by substituting $E_F \rightarrow E$,

$$\tilde{\eta}_i(E) \equiv \sum_{n\mathbf{k}} \left| \langle n, \mathbf{k} | \frac{\partial V_{SCF}}{\partial \mathbf{R}_i} | n, \mathbf{k} \rangle \right|^2 \delta(E - E_{n\mathbf{k}}). \quad (21)$$

This expression has the form of a density of states weighted by the sensitivity of the electronic states to atomic displacements. Whereas $\lambda = 0$ and $\tilde{\eta}_i(E_F) = 0$ for all non-metallic materials, $\tilde{\eta}_i(E)$ will have non-zero values and potentially interesting features for all materials. By looking at this coupling parameter as a function of energy, we can immediately examine rigid-band doping scenarios and get a better sense of the magnitude of hypothetical electron-phonon couplings.

The effects of anisotropy have been considered in deriving $\tilde{\eta}_i$, but so far neglected is phonon anharmonicity, which can be of equal importance in materials such as MgB₂¹⁵. Anharmonicity is important for "soft" phonon modes where the average displacement of atoms is large enough that it samples the non-harmonic terms of the potential energy surface. Eliashberg theory can be formally reformulated to account for anharmonicity²⁰, where the largest effect is typically an increase in phonon frequencies and other corrections contain multi-phonon processes and Debye-Waller factors. The most common approach taken is the inclusion of anharmonic phonon frequencies wherever phonon frequencies appear in Eliashberg theory. At this level of correction, $\tilde{\eta}_i$ and thus the quantity $\tilde{\lambda}\langle\tilde{\omega}^2\rangle$ are unchanged as they are independent of the phonon spectrum. Anharmonic corrections can of course shift the average phonon frequency $\langle\tilde{\omega}^2\rangle$, but $\tilde{\lambda}$ will correspondingly change such that their product remains constant. Taking into account more anharmonic effects, $\tilde{\eta}_i$ can also change because V_{SCF} in Eq. (20) is dependent on atomic positions and will be affected by large atomic displacements. The anharmonic phonon frequency correction is significant because as a phonon softens the harmonic change in energy with phonon displacement, $d^2E/d\xi^2$, gets small and the phonon frequency becomes dominated by anharmonic corrections proportional to $(d^4E/d\xi^4)\Delta R^2$, where ΔR is the magnitude of the average phonon mode displacement. In contrast, the anharmonic $\tilde{\eta}_i$ correction typically will not be important because the harmonic value does not get small as phonons soften and as is shown in section IV, one mechanism of phonon softening is actually related to large $\tilde{\eta}_i$ values. The only anharmonic effects we will consider are corrections to $\langle\tilde{\omega}^2\rangle$ and not $\tilde{\eta}_i$.

To calculate $\tilde{\eta}_i(E)$ using a modern electronic structure code, we must find an approximation to $\partial V_{SCF}/\partial \mathbf{R}_i$ in

Eq. (21). The potential due to the displacement of a single atom in a crystal breaks translational symmetry and is a difficult quantity to compute using codes that rely on periodicity. A reasonable approximation to this single atom displacement is the displacement of a single atom per unit cell within a sufficiently large supercell of the material of interest. This displacement is a zone-center perturbation and the matrix elements in Eq. (21) are simply obtained from first order perturbation theory on the band energies,

$$\tilde{\eta}_i(E) = \sum_{n\mathbf{k}} \left| \frac{\partial E_{n\mathbf{k}}}{\partial \mathbf{R}_i} \right|^2 \delta(E - E_{n\mathbf{k}}). \quad (22)$$

This calculation is no more difficult than decomposing the force on each atom into its individual band and k -point contributions and then calculating a density of states. The $\tilde{\eta}_i$ obtained from this procedure does not require the rigid-muffin-tin approximation (RMTA) often made in other more simplified calculations of electron-phonon coupling^{21,22}. By utilizing a supercell approximation, we assume spatial locality of electron-phonon coupling as in the RMTA, but here this assumption can be systematically verified and improved by increasing the size of the supercell. The calculations in this paper are performed using the PWSCF electronic structure code²³ with the provided default norm-conserving pseudopotentials and converged plane-wave cutoffs. Unless otherwise noted, calculations are performed with experimental lattice constants. Density of states and $\tilde{\eta}_i(E)$ calculations are performed using gaussian smearing and $\partial E_{n\mathbf{k}}/\partial \mathbf{R}_i$ values based on multiple calculations with displaced atomic coordinates and a finite difference approximation. The gaussian smearing width and k -point grid utilized in each calculation are noted with the results. The $\tilde{\eta}_i(E)$ values depend on the choice of unit cell, and for easier comparison we use a unit cell-independent $\tilde{\eta}(E)$ value that is summed over the atoms in the unit cell. The summed $\tilde{\eta}(E)$ value can be used in Eq. (19) with an appropriate average atomic mass. As an example, we calculate $\tilde{\eta}(E)$ for diamond in figure 2. Within the precision of the calculation, there is no difference between $\tilde{\eta}(E)$ calculated in one unit cell and in a $2 \times 2 \times 2$ supercell. This demonstrates the locality of the electron-phonon coupling that results from a strong covalent bond. Because a large supercell isn't required for accurate $\tilde{\eta}(E)$'s, this is a computationally efficient methodology for calculating electron-phonon couplings in systems of this type.

Based on this analysis, we can now write T_c in the strongly coupled limit as

$$T_c \sim \sqrt{N(E_F)} \sum_i \frac{F_i^{FS}}{\sqrt{M_i}}, \quad (23)$$

where F_i^{FS} is the average root-mean-square force on atom i from electrons on the Fermi surface. This relation reflects the common wisdom based on the BCS model that a large density of states at E_F and light elements are what lead to a high T_c . It also helps to give a

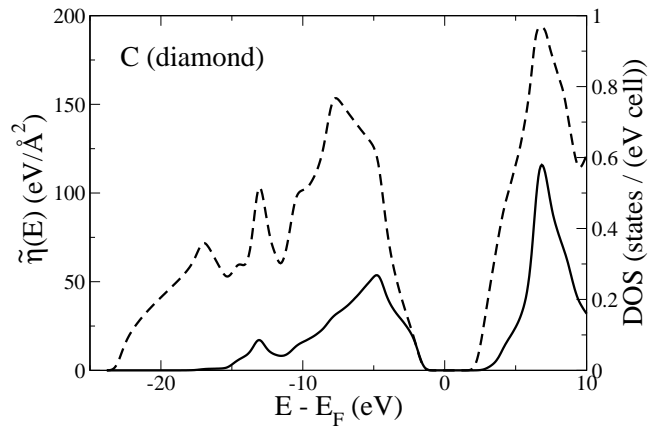


FIG. 2: Density of states (DOS) (dashed line) and $\tilde{\eta}(E)$ (solid line) for diamond. This calculation is performed on one unit cell of diamond with a $24 \times 24 \times 24$ k -grid and 0.03 Rydberg

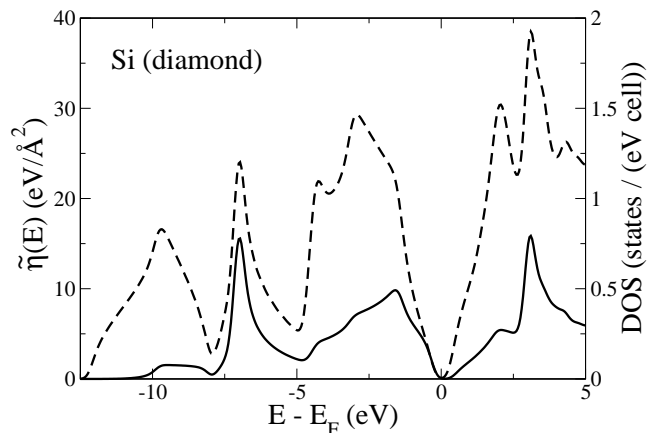


FIG. 3: Density of states (dashed line) and $\tilde{\eta}(E)$ (solid line) for silicon in the diamond structure. This calculation is performed on one unit cell with a $24 \times 24 \times 24$ k -grid and 0.015 Rydberg gaussian smearing.

simple qualitative picture of electron-phonon coupling by allowing us to focus on a single electronic state and atom at a time. If the electron occupies a single orbital of this atom, its charge distribution will be symmetric about the atomic center and it will contribute no net force to the atom. This is related to the $l \rightarrow l' \pm 1$ angular momentum sum rule in the electron-phonon coupling calculations of Hopfield²⁴. Nonzero coupling arises from deviations from spherical symmetry around an atom and the length scale for this deviation is the inter-atomic spacing. In terms of a tight-binding model with inter-atom hopping parameter t , we can use a simple chain rule argument to relate $\tilde{\eta}$ to t , $dE/d\mathbf{R} = (dE/dt)(dt/d\mathbf{R})$, whereby a atomic displacement perturbs the neighboring hopping parameters and they in turn perturb the band energies. Strong electron-phonon coupling is related to a large sensitivity

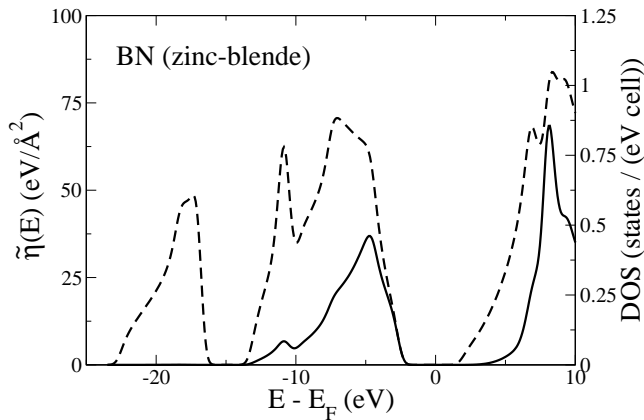


FIG. 4: Density of states (dashed line) and $\tilde{\eta}(E)$ (solid line) for cubic boron nitride. This calculation is performed on one unit cell with a $24 \times 24 \times 24$ k-grid and 0.03 Rydberg gaussian smearing. In a single unit cell approximation, $\tilde{\eta}_i(E)$ is

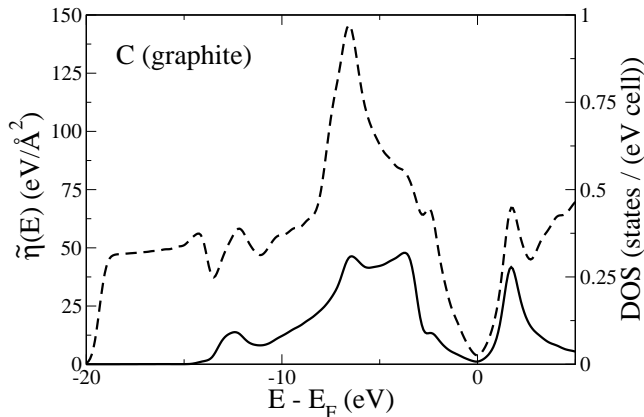


FIG. 5: Density of states (dashed line) and $\tilde{\eta}(E)$ (solid line) for graphite. This calculation is performed on one unit cell of AA-stacked graphite with a $24 \times 24 \times 12$ k-grid and 0.03 Rydberg gaussian smearing. Only in-plane motions of the carbon atoms are considered; the out of plane motions do not contribute significantly to $\tilde{\eta}(E)$.

in t with respect to atomic displacements, $dt/d\mathbf{R}$, and not directly to a large t .

To study the effects of covalent bonding on electron-phonon coupling, we compare $\tilde{\eta}(E)$ values of several related materials. As an example of changing bond length and strength, we compare the $\tilde{\eta}(E)$ of diamond in figure 2 with silicon in a diamond structure in figure 3. Carbon has $\tilde{\eta}(E)$ values between two and ten times larger than silicon presumably due to a shorter, stronger covalent bond and less core screening. The density of states of silicon is twice that of carbon and within a tight-binding picture this is associated with a factor of two reduction in t . Although we generally associate larger λ values to larger density of states values at the Fermi surface, this

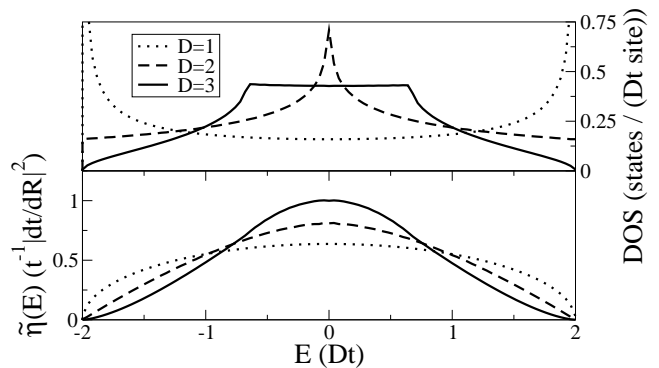


FIG. 6: Density of states and $\tilde{\eta}(E)$ for simple cubic tight binding in $D=1,2,3$ dimensions.

reduction in t is concurrent with a reduction in $dt/d\mathbf{R}$ that leads to an overall decrease in $\tilde{\eta}(E)$. We can next examine the effect of bond ionicity on $\tilde{\eta}$ by comparing diamond with boron nitride in a zinc-blende structure in figure 4. Although their bond lengths are very similar, boron nitride has a more ionic, less covalent bond than diamond and the $dt/d\mathbf{R}$ and η values are correspondingly reduced. All these materials share the diamond (zinc-blende) structure and contain similar peaks in $\tilde{\eta}(E)$ above and below the Fermi level, due to strong coupling associated with the anti-bonding and bonding states respectively.

Besides changes in bond strength and ionicity, we can also change the character of a covalent bond by changing the structure of a system. Carbon in graphite has sp^2 bonding instead of the sp^3 bonding of the diamond structure. In this structure there are only three bonds per atom rather than four in diamond, but the bond lengths are shorter and the bonds are stronger. In figure 5 we plot the density of states and $\tilde{\eta}(E)$ of graphite. The $\tilde{\eta}(E)$ for valence states of diamond and graphite are more similar in shape and magnitude than their density of states. The biggest difference in valence electron-phonon coupling between these systems is the peak in coupling of diamond being replaced by a smaller, wider plateau in graphite. The features of $\tilde{\eta}(E)$ do not directly correspond to density of states features in the diamond-structure examples, and the deviation is even more pronounced in graphite. In particular, the maximum in the valence density of states of graphite associated with a van Hove singularity of graphene is not associated with a maximum in electron-phonon coupling.

To understand the fundamental difference between $N(E)$ and $\tilde{\eta}(E)$, we calculate both for a simple cubic nearest-neighbor tight binding model with no on-site energy and a hopping energy t in one, two, and three dimensions. Electron-phonon coupling is modeled by assuming that atomic displacements at a site correspond to changes in hoppings from that site parameterized by a constant $dt/d\mathbf{R}$ dotted with the unit normal vector in the direction of the hopping. The $N(E)$ and $\tilde{\eta}(E)$ of these

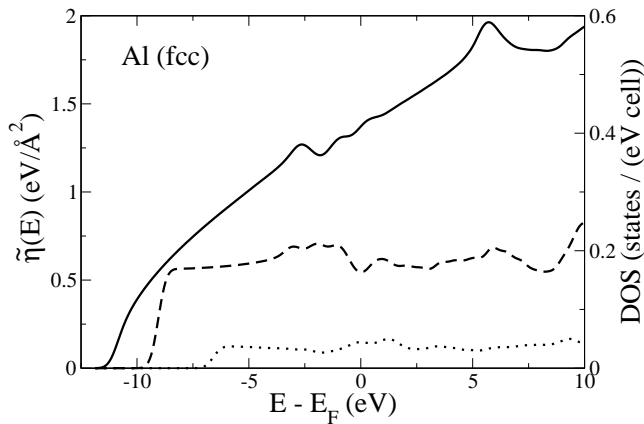


FIG. 7: Density of states in the primitive cell (solid line) and $\tilde{\eta}(E)$ of fcc aluminum for a $2 \times 2 \times 2$ supercell with an $18 \times 18 \times 18$ k-grid (dotted line) and a $3 \times 3 \times 3$ supercell with a $12 \times 12 \times 12$ k-grid (dashed line). The experimental value of η at E_F is $2 \text{ eV}/\text{\AA}^2$.

three systems are plotted in figure 6, showing that van Hove singularities characteristic of low dimensionality do not cause divergences of $\tilde{\eta}(E)$. The shape of $\tilde{\eta}(E)$ is relatively insensitive to dimensionality and is proportional in all cases to a generic tight binding result,

$$\tilde{\eta} \sim \frac{1}{t} \left| \frac{dt}{d\mathbf{R}} \right|^2. \quad (24)$$

This result suggests that the traditional decomposition of the electron-phonon coupling parameter λ into $N(E_F)V_{ep}$ is possibly misleading in the vicinity of band edges and van Hove singularities.

In metallic systems without covalent bonding, there is a significant convergence problem in our method for calculating $\tilde{\eta}(E)$. For example in a simple metal such as aluminum, as shown in figure 7, we cannot converge an answer with respect to either k-point sampling or supercell size. The physical phenomenon causing this problem is that charge density changes in a metal such as the displacement of an atom lead to long range Friedel oscillations which are difficult to sample with the necessary precision. The magnitude of the electron-phonon coupling associated with this phenomenon is much smaller than the coupling due to strong covalent bonds. Any sampling errors associated with Friedel oscillations are negligible in systems with larger electron-phonon coupling contributions coming from covalent bonds.

There is a large variation of electron-phonon coupling in the examples studied, a factor of five increase in the maximum of $\tilde{\eta}(E)$ in going from aluminum to silicon and another factor of five increase in carbon over silicon. These variations of magnitude can be approximately reproduced based on scaling arguments. The first approximation we make is to assume that $\partial E_{n\mathbf{k}}/\partial \mathbf{R}_i$ in Eq. (22) is independent of n and \mathbf{k} variations. This allows us to separate out the $n\mathbf{k}$ sum and equate it to the density

of states per spin times the variation in the electronic energy,

$$\tilde{\eta}_i(E) \approx N_{\uparrow}(E) \left| \frac{\partial E_{el}}{\partial \mathbf{R}_i} \right|^2. \quad (25)$$

The sensitivity of electronic energy to atomic displacements is approximately related to the hydrostatic deformation potential - the sensitivity of electronic energy to change in the volume of the unit cell times the volume - divided by a length scale, in this case the bond length. In a free electron gas, the standard result²⁵ for the hydrostatic deformation potential is $\frac{2}{3}E_F$. Our simple model for $\tilde{\eta}(E)$ is thus

$$\tilde{\eta}(E) \approx \frac{4}{9}N_{\uparrow}(E) \left(\frac{E_F}{R_{bond}} \right)^2. \quad (26)$$

The $N_{\uparrow}(E)$ is taken from figures 2 and 3 at the maximum of $\tilde{\eta}(E)$ and from figure 7 at E_F . The value of E_F in this model is taken to be the bandwidth of occupied valence states again taken from the figures: 22 eV for carbon, 15 eV for silicon, and 12 eV for aluminum. With the experimental bond lengths, we get $\tilde{\eta}_{max}$ values of 27 eV/ \AA^2 for carbon, 11 eV/ \AA^2 for silicon, and 1.6 eV/ \AA^2 for aluminum. While these values are not quantitatively correct, they reasonable reproduce the trend of increasing electron-phonon coupling in these three materials. The large variations in $\tilde{\eta}$ are just magnifications of the variations in bond lengths and strengths.

The possibility of a high T_c becomes more probable with increasing $\tilde{\eta}_i(E)$ and decreasing M_i for the atoms constituting a material. In going from silicon to carbon in a diamond structure we see that both these parameters favor the lighter element. The lightest elements that can form strong covalent bonds under ambient conditions are hydrogen, beryllium, boron, carbon, nitrogen, oxygen, and fluorine. These are the elements that should make up the covalent framework central to the idea of a covalent metal superconductor. A hypothetical covalent metal superconductor need not exclude other elements; they might play a role as dopants or be themselves bonded to one of the strong covalent elements. This encompasses a broad class of materials, but two important considerations must guide and constrain the search for strong electron-phonon coupling. The features of $\tilde{\eta}(E)$ associated with covalent bonds are peaked in a relatively narrow range of energies. Bonds between different pairs of elements of different lengths and strengths will contribute to $\tilde{\eta}(E)$ at different energies. Only electrons at the Fermi energy can contribute to the superconducting state, therefore it is important to choose a material with bonds that primarily contribute their electron-phonon coupling to one energy. Additionally, if a material has bonds of different strengths, the weakest bonds will typically have their bonding and anti-bonding states closest to the undoped Fermi level. If the Fermi level change required to bring $\tilde{\eta}(E_F)$ to the strong bonding (anti-bonding) states crosses weaker bonding (anti-bonding)

states, it might sufficiently deplete (fill) the weak bond enough to break it and destabilize the material. In some cases this problem can be averted by shifting the relative energy levels of bonds through charge transfer such as that which occurs with the σ and π states of MgB_2 ²⁶.

For a given material we can now roughly bound the maximum possible T_c by rigidly shifting the Fermi level and using $\tilde{\eta}(E)$, Eq. (19), and Eq. (10) to tune to the largest T_c . There are several caveats to this approach, the primary one being that synthesizing heavily doped materials can be very difficult. This difficulty arises from the presence of more energetically favorable structures or structural instability in the candidate material. Even if it is possible to physically modify a system and effectively shift its Fermi level, the modification might also change $\tilde{\eta}(E)$ from its initial value, for better or worse. An additional problem arises in molecular crystals where weakening intermolecular hopping and narrow bands can cause a divergence in both $N(E)$ and $\tilde{\eta}(E)$ and a breakdown of Eliashberg theory. In the case of doped C_{60} solids, it is believed²⁷ that non-adiabatic effects and a Mott insulator transition are required to fully account for some observed behavior. These are electronic effects beyond the scope of this paper that potentially bound T_c by electronic energy scales. More relevant to non-molecular crystals with a wider electronic bandwidth, we next examine a fundamental instability of the phonon-mediated superconducting state that bounds T_c by a smaller, phonon energy scale.

IV. PHONON SOFTENING

The phonon softening due to electron-phonon interactions can lead to a structural instability that sets an upper limit to the possible T_c of a material. Phonon softening is defined as a change in phonon frequencies from some well-defined bare frequency to the actual frequencies present in a material. The early research on phonon softening took the bare phonons to be of purely electrostatic origin, as either coming from a screened ion-ion interaction⁹ or the ions and frozen valence electrons⁷. A recent study¹⁰ has included quantum effects in the definition of the bare phonons, using metallic screening with an insulating electronic susceptibility. Since superconductivity is the result of interactions between phonons and electrons near the Fermi surface, we will define the bare phonon frequencies here by isolating and removing all electronic contributions to phonon frequencies coming from the Fermi surface.

To calculate the phonon spectrum of a material we must first consider its dynamical matrix,

$$D_{ij}^{\alpha\beta} \equiv \frac{\partial^2 E}{\partial R_i^\alpha \partial R_j^\beta} = \frac{\partial^2 E_{ion-ion}}{\partial R_i^\alpha \partial R_j^\beta} + \int \rho_{el}(\mathbf{r}) \frac{\partial^2 V_{ion}(\mathbf{r})}{\partial R_i^\alpha \partial R_j^\beta} d\mathbf{r} + \int \frac{\partial \rho_{el}(\mathbf{r})}{\partial R_i^\alpha} \frac{\partial V_{ion}(\mathbf{r})}{\partial R_j^\beta} d\mathbf{r}, \quad (27)$$

where i, j are the atom indices and α, β are the Cartesian coordinate indices. The first two terms are the classical electrostatic contribution between ions and a fixed electronic charge background, while the third contains contributions coming from the electronic response. All Fermi surface contributions are contained within the third term of the dynamical matrix, and we rewrite it in a more symmetric manner using the chain rule,

$$\int \frac{\partial \rho_{el}(\mathbf{r})}{\partial R_i^\alpha} \frac{\partial V_{ion}(\mathbf{r})}{\partial R_j^\beta} d\mathbf{r} = \int \frac{\partial V_{ion}(\mathbf{r}')}{\partial R_i^\alpha} \frac{\partial \rho_{el}(\mathbf{r}')}{\partial V(\mathbf{r}')} \frac{\partial V_{ion}(\mathbf{r}')}{\partial R_j^\beta} d\mathbf{r}' d\mathbf{r}'. \quad (28)$$

The middle term, $\partial \rho / \partial V$, is the electron susceptibility, usually denoted as χ , that quantifies the response of the electron density to a change in the background potential. If the contribution to χ due to the Fermi surface is small, then it can be related to the Fermi surface contribution to the irreducible susceptibility χ_0 through perturbation theory²⁸,

$$\Delta \chi^{FS} \approx \epsilon^{-\dagger} \Delta \chi_0^{FS} \epsilon^{-1}, \quad (29)$$

where ϵ^{-1} is the inverse dielectric function of the material and $\epsilon^{-\dagger}$ is its Hermitian conjugate. The irreducible susceptibility can be expressed analytically in terms of electronic states,

$$\chi_0(\mathbf{r}, \mathbf{r}') = 2 \sum_{n\mathbf{k}, n'\mathbf{k}'} \langle n\mathbf{k} | \mathbf{r} \rangle \langle \mathbf{r} | n'\mathbf{k}' \rangle \langle n'\mathbf{k}' | \mathbf{r}' \rangle \langle \mathbf{r}' | n\mathbf{k} \rangle \times \frac{f_{n'\mathbf{k}'} - f_{n\mathbf{k}}}{E_{n'\mathbf{k}'} - E_{n\mathbf{k}}}, \quad (30)$$

for Fermi occupations $f_{n\mathbf{k}}$. The susceptibility contains contributions from all pairs of electronic states, and to restrict these pairings to the vicinity of the Fermi surface we introduce energy cutoffs, $E_F - \Delta E \leq E \leq E_F + \Delta E$, to both sums over states. For sufficiently small ΔE , the second term in Eq. (30) can be approximated by $df_{n\mathbf{k}}/dE$, which can in turn be approximated by $-\delta(E_F - E_{n\mathbf{k}})$ for sufficiently low temperatures. With this as our expression for $\Delta \chi_0^{FS}$, we can now approximate the contribution of the Fermi surface electrons to the dynamical matrix using Eq. (29) and Eq. (28),

$$\Delta D_{ij}^{\alpha\beta, FS} \approx -2 \sum_{n\mathbf{k}, n'\mathbf{k}'} \langle n, \mathbf{k} | \frac{\partial V_{SCF}}{\partial R_i^\alpha} | n', \mathbf{k}' \rangle \times \langle n', \mathbf{k}' | \frac{\partial V_{SCF}}{\partial R_j^\beta} | n, \mathbf{k} \rangle \delta(E_F - E_{n\mathbf{k}}) \times \theta((\Delta E)^2 - (E_F - E_{n'\mathbf{k}'})^2). \quad (31)$$

Here, the screened self-consistent potentials are the result of the inverse dielectric function acting on the bare ionic potentials,

$$\frac{\partial V_{SCF}}{\partial R_i^\alpha} = \epsilon^{-1} \frac{\partial V_{ion}}{\partial R_i^\alpha}, \quad (32)$$

and θ is the unit step function.

As $\Delta E \rightarrow 0$, the ΔD^{FS} term vanishes. The Fermi surface does not have an infinitesimal effect on phonon frequencies, but rather it affects an infinitesimal number of phonons. For a phonon of wavevector \mathbf{q} , we would calculate the softening due to the Fermi surface by taking the expectation value of ΔD^{FS} with respect to the phonon displacement vector. This leads to a substitution in Eq. (31) of $\mathbf{k}' \rightarrow \mathbf{k} + \mathbf{q}$ due to momentum conservation. For sufficiently small \mathbf{q} or in special cases of Fermi surface nesting, the condition $|E_F - E_{n(\mathbf{k}+\mathbf{q})}| \leq \Delta E$ holds for \mathbf{k} over a finite area of the Fermi surface and lead to finite phonon softening. As ΔE is made larger, more phonons will be softened by ΔD^{FS} but the approximations made in deriving Eq. (31) eventually break down and the correspondence with electrons at the Fermi surface is lost. All the electrons in a material can play a role in softening the phonon frequencies from the ionic plasma frequencies, and the Fermi surface is not independent of the rest of the electronic structure. These additional phonon softening effects are not directly related to the Fermi surface and must be handled separately for different classes of materials. For example, in metallic $\text{Li}_{1-x}\text{BC}^{29,30}$ there is an essentially constant softening for phonons from $\mathbf{q} = 0$ to $|\mathbf{q}| = 2k_F$. We imagine that for a hypothetical well-engineered superconductor, all material-specific phonon softening is designed so that it doesn't lead to any structural instabilities, leaving only ΔD^{FS} as the fundamentally limiting cause of phonon instability.

With several more manipulations, the phonon softening due to electron-phonon coupling can be directly related back to a bound on T_c . We first relate ΔD^{FS} to the softening of an individual phonon mode with displacement vector ξ_i^α ,

$$(\Delta\omega^2)^{FS} = \sum_{i\alpha, j\beta} \frac{\xi_i^\alpha}{\sqrt{M_i}} \Delta D_{ij}^{\alpha\beta, FS} \frac{\xi_j^\beta}{\sqrt{M_j}}. \quad (33)$$

Summing over all phonon modes at the gamma point, we have a complete basis of gamma point atomic displacements and can relate the phonon softening back to the total electron phonon coupling,

$$\sum_i (\Delta\omega_i^2)^{FS} \approx 2\tilde{\lambda}\langle\tilde{\omega}^2\rangle, \quad (34)$$

assuming $\tilde{\eta}_i$ has been calculated using Eq. (22) within the supercell approximation. This leads to a bound on T_c by invoking the weak upper bound of Eq. (7) to get

$$T_c \leq 0.13 \sqrt{\sum_i (\Delta\omega_i^2)^{FS}}. \quad (35)$$

This phonon softening T_c bound gets large as more phonons are softened and as the magnitude of the softening increases. However, the total phonon softening is related to the total electron-phonon coupling strength, which is itself independent of the phonon spectrum.

Phonon softening becomes the relevant bound on T_c only when there is enough electron-phonon coupling in a material to drive a phonon mode to instability before the electron-phonon coupling strength is maximized. The identification of this one ‘‘Achilles’ heel’’ mode and its subsequent destabilization are required to correctly interpret Eq. (35). The degree to which a phonon mode can even be softened by the Fermi surface has to do with its overlap in Eq. (33) with ΔD^{FS} ; one has to evaluate these overlaps to determine the relative softening of various phonon modes. This ‘‘Achilles’ heel’’ might not even be determined by softening due to electrons at the Fermi surface - other valence electrons and physical modifications required to dope a material might both play an important material-specific role in the softening of phonons. A caveat to this phonon softening argument is that it has been made based on the harmonic phonon approximation which will cease to hold if some phonon modes are sufficiently softened. Anharmonic corrections to phonon frequencies can stabilize locally unstable modes, further delaying the onset of a true instability and raising the associated T_c bound.

A simple application of Eq. (35) is the case of diamond. In diamond, the gamma point has three zero frequency acoustic modes and three equal frequency optical modes at the gamma point. The maximum phonon softening allowed in a stable structure is full softening to zero of the optical modes. The gamma point optical modes have an experimentally measured frequency of 165 meV³¹, which from Eq. (35) gives a T_c bound of 430 K. According to figure 2, the maximum T_c possible with rigid hole doping is 290 K and with electron doping it is 420 K. Within a rigid doping scheme, the theoretical limit of superconductivity in diamond is set by the amount of available electron-phonon coupling and not by a fundamental lattice instability, due to the extreme stiffness of the undoped structure.

V. T_c BOUNDS OF COVALENT METALS

Originating from the discovery of superconductivity in MgB_2 in 2001⁵, there has been a growing interest in covalent metals. One goal of this area of research is to determine, if possible, how to increase T_c in already superconducting materials and how to drive insulating covalent materials into a metallic, superconducting regime. The most prominent materials in these studies are two layered materials, metallic MgB_2 and semiconducting (at $x = 0$) Li_{1-x}BC , and one isotropic material, boron-doped diamond B_xC_{1-x} . The $\tilde{\eta}_i(E)$ -based analysis derived in section III provides a clear picture of the T_c bounds inherent in these materials.

In MgB_2 , neither hole-doping nor electron-doping have been successful in increasing T_c ¹⁰. This has been explained theoretically in terms of the magnitude of the phonon softening of the E_{2g} phonon mode as a function of doping level. Because it is near to the strongly

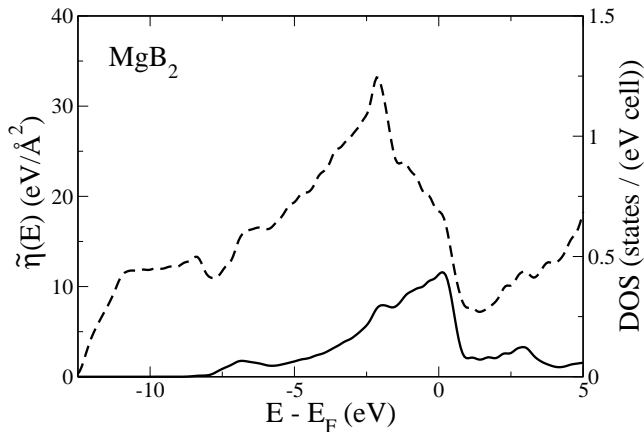


FIG. 8: Density of states (dashed line) and $\tilde{\eta}(E)$ (solid line) for MgB_2 . This calculation is performed on one unit cell with a $24 \times 24 \times 24$ k-grid and 0.03 Rydberg gaussian smearing. Only in-plane motions of the boron atoms are considered; the out of plane boron motions and magnesium atoms do not contribute significantly to $\tilde{\eta}(E)$ in the valence bands.

coupled regime, $\lambda \approx 1$, the variation of T_c with doping should follow $\tilde{\eta}(E)$, shown in figure 8. This figure clearly shows that MgB_2 is an optimally doped superconductor and that T_c should dramatically decrease with electron-doping and gradually decrease with hole-doping, which accurately reproduces the results of Zhang et al¹⁰. As for the magnitude of T_c at optimal doping, our calculation gives $T_c = 29 \sim 39$ K using the Einstein spectrum T_c formula of Eq. (10) with $\mu^* = 0.1 \sim 0.15$ and $\tilde{\lambda} = 0.75$ determined by setting $\sqrt{\langle \tilde{\omega}^2 \rangle} = 76$ meV, the anharmonic frequency of the E_{2g} phonon mode³². This range of T_c values encompasses the experimental value of 39 K for a physical range of μ^* values.

In LiBC, it has been predicted that superconductivity will occur upon uniform deintercalation of the lithium to the level of greater than $\sim 10\%$ and T_c will plateau at $\sim 50\%$ deintercalation with values as low as 65 K³⁰ and as high as 100 K³³. The plot of $\tilde{\eta}(E)$ for LiBC in figure 9 shows a magnitude of electron-phonon coupling twice that of MgB_2 in figure 8 but less than half that of graphite in figure 5. Upon hole doping to the peak of $\tilde{\eta}(E)$ in the valence states, we predict a transition temperature in the range $T_c = 90 \sim 100$ K using the Einstein spectrum T_c formula of Eq. (10) with $\mu^* = 0.1 \sim 0.15$ and $\tilde{\lambda} = 1.6$ determined by setting $\sqrt{\langle \tilde{\omega}^2 \rangle} = 85$ meV, the calculated frequency of the E_{2g} phonon mode after doping²⁹ (softened from 150 meV). The broad plateau in $\tilde{\eta}(E)$ for a wide range of doping levels corresponds to the T_c plateau found in prior predictions^{30,33}. An experimental method for removing lithium or synthesizing lithium-deficient LiBC without degrading the structure has not yet been discovered and remains the barrier to fulfilling these predictions.

In diamond, it has been observed that heavy boron

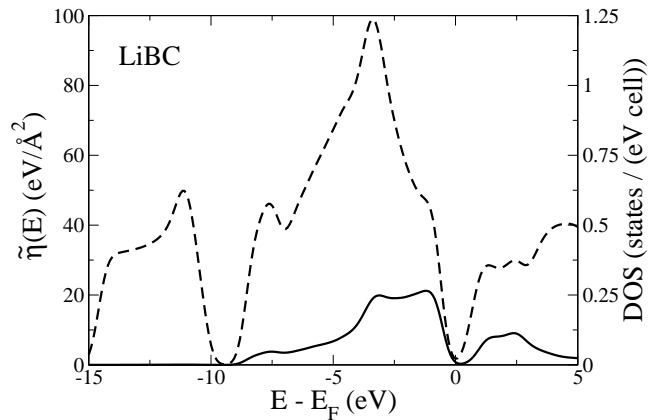


FIG. 9: Density of states (dashed line) and $\tilde{\eta}(E)$ (solid line) for LiBC. DOS is scaled to half the actual $(\text{LiBC})_2$ unit cell to be comparable to the unit cells of AA-stacked graphite and MgB_2 . This calculation is performed on one unit cell with a $24 \times 24 \times 12$ k-grid and 0.03 Rydberg gaussian smearing. Only in-plane motions of the boron and carbon atoms are considered; their out of plane motions and lithium atoms do not contribute significantly to $\tilde{\eta}(E)$ in the valence bands. In a single unit cell approximation, $\tilde{\eta}_i(E)$ is identical for boron

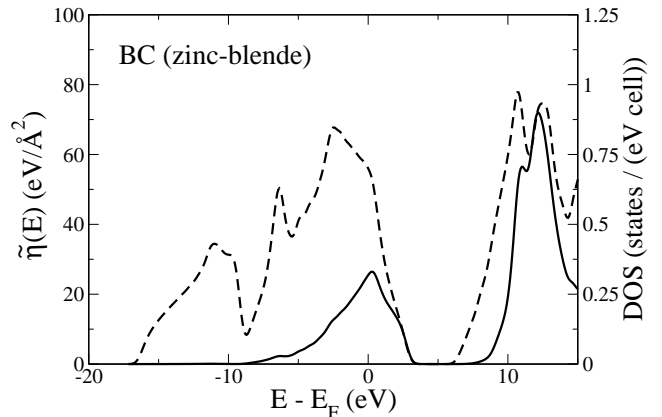


FIG. 10: Density of states (dashed line) and $\tilde{\eta}(E)$ (solid line) for zinc-blende boron carbide. This calculation is performed on one unit cell with a $24 \times 24 \times 24$ k-grid and 0.03 Rydberg gaussian smearing. The equilibrium lattice constant is calculated to be 3.72 Å. In a single unit cell approximation, $\tilde{\eta}_i(E)$ is identical for boron and carbon.

doping, up to the solubility limit, leads to superconductivity with $T_c \approx 4$ K in bulk diamond³⁴ and $T_c \approx 9$ K in diamond thin films³⁵. This doping level corresponds to $\sim 3\%$ boron substitution and is still far from the optimal value of 50% boron substitution estimated from integrating the DOS from E_F to the valence band peak of $\tilde{\eta}(E)$ in figure 2. A small unit cell material corresponding to this optimal doping level is BC in a zinc-blende structure, which has been examined previous in the context of material strength³⁶. We calculate $\tilde{\eta}(E)$ for zinc-blende BC

in figure 10 and verify the optimal doping, but there is a substantial drop in the overall scale of electron-phonon coupling from the strong C-C bonds in diamond to the weaker B-C bonds. The scale of the electron-phonon coupling is comparable to the graphitic sheets of boron and carbon in LiBC, but the peak in the zinc-blende structure is narrower and $\sim 20\%$ higher. This material is stable, unlike BC in a graphitic structure, with a dramatic softening of the gamma point optical mode from 165 meV in diamond to a calculated value of 55 meV in BC. This phonon calculation is performed using the frozen phonon method with anharmonic corrections; the total energy as a function of phonon displacement is fit to a 6th order polynomial and the frequency is calculated as the energy difference between the first excited state and ground state of the associated anharmonic oscillator. From the calculated phonon frequency, we get $\tilde{\lambda} = 3.6$ and using the Einstein spectrum T_c formula of Eq. (10) with $\mu^* = 0.1 \sim 0.15$, we predict the transition temperature of this material to be in the range $T_c = 140 \sim 160$ K. The barrier to reaching T_c values of this magnitude in diamond is the difficulty of including boron into the material beyond the solubility limit and the formation of boron-based impurities that don't act as acceptors³⁷.

A recent study³⁸ has examined the possibility of electron-doping in diamond, which they conclude might lead to larger T_c values than hole-doping. This study was based on small doping levels, less than 6%, and we continue this argument to the doping limits. The $\tilde{\eta}(E)$ peak in the conduction band of diamond is more than twice as large as the valence peak, but requires significantly more doping to reach. Electron-doping is presumed to be achieved by nitrogen substitution and a material representative of 50% doping is CN in a zinc-blende structure, which is known to be structurally unstable³⁹. The $\tilde{\eta}(E_F)$ of zinc-blende CN is smaller than in zinc-blende BC and still far from the peak in the conduction band. We conclude from this that hole doping is the best prospect for exploring the limits of T_c in superconducting diamond.

VI. CONCLUSIONS

The phonon frequency being a bound on T_c is an obvious conclusion from the weak coupling limit of conventional electron-phonon superconductivity. It takes a great deal more effort to show that this is still a bound in the strong coupling limit where T_c at first glance appears

not to have a bound. This bound is caused by the softening of phonon modes to instability due to strong electron-phonon coupling. In a simplified Eliashberg framework, the variation with doping and hypothetical maximum of electron-phonon coupling can be studied through a single efficiently calculable metric, $\tilde{\eta}(E)$. In a material with strong covalent bonds, such as diamond, we can see that the T_c bound due to softening cannot be reached because there is not enough electron-phonon coupling strength available to soften the phonons to instability. In such a material, an upper bound on T_c is set by the maximum available electron-phonon coupling.

Of the materials studied, only MgB₂ has maximized its electron-phonon coupling within an as-yet experimentally realizable material. Careful materials design and synthesis will be required to increase the maximum available electron-phonon coupling and approach the T_c limits set by structural stability. For some materials containing carbon-carbon and equally strong bonds and light atomic masses, this T_c limit is higher than room temperature. These hypothetical materials are likely to need weak links to enhance $N(E_F)$ and therefore $\tilde{\eta}(E_F)$ and interstitial regions to contain donor or acceptor atoms or molecules that don't play a role in the stability of the lattice and can be removed or added to chemically dope the covalent network into a metallic regime. Molecular crystals fit this description, but intermolecular hopping is often too weak and prevents conduction. Polymerization of some of the constituent molecules might serve to increase hopping and enhance conduction. These criteria constitute a broad class of hypothetical materials, and further theoretical progress can be directed and stimulated by the experimental realization of such materials - much as the recent interest in phonon-mediated superconductivity in covalent metals has been motivated by the discovery of superconductivity in MgB₂.

Acknowledgments

This work was supported by National Science Foundation Grant No. DMR04-39768 and by the Director, Office of Science, Office of Basic Energy Sciences, Division of Materials Sciences and Engineering Division, U.S. Department of Energy under Contract No. DE-AC02-05CH11231.

Calculations in this work have been done using the Quantum-ESPRESSO package²³.

* Electronic address: jmoussa@civet.berkeley.edu

¹ M. L. Cohen and P. W. Anderson, in *Superconductivity in d- and f-Band Metals*, edited by D. H. Douglass (AIP, New York, 1972), p. 17.

² W. L. McMillan, Phys. Rev. **167**, 331 (1968).

³ P. B. Allen and R. C. Dynes, Phys. Rev. B **12**, 905 (1975).

⁴ O. V. Dolgov, D. A. Kirzhnits, and E. G. Maksimov, Rev. Mod. Phys. **53**, 81 (1981).

⁵ J. Nagamatsu, N. Nakagawa, T. Muranaka, Y. Zenitani and J. Akimitsu, Nature (London) **410**, 63 (2001).

⁶ P. B. Allen and M. L. Cohen, Phys. Rev. Lett. **29**, 1593 (1972).

- ⁷ P. B. Allen and R. C. Dynes, Phys. Rev. B **11**, 1895 (1975).
- ⁸ W. E. Pickett and P. B. Allen, Phys. Rev. B **16**, 3127 (1977).
- ⁹ I. R. Gomersall and B. L. Gyorffy, Phys. Rev. Lett. **33**, 1286 (1974).
- ¹⁰ P. Zhang, S. G. Louie, M. L. Cohen, Phys. Rev. Lett. **94**, 225502 (2005).
- ¹¹ C. R. Leavens, J. Phys. F **7**, 1911 (1977).
- ¹² The $dT_c/d\alpha^2 F(\omega)$ response for fixed λ and $\langle\omega^2\rangle$ is numerically calculated to be positive in the frequency interval from zero to ω_{max} .
- ¹³ G. Varelogiannis, Phys. Rev. B **51**, 3941 (1995).
- ¹⁴ H. Suhl, B. T. Matthias, and L. R. Walker, Phys. Rev. Lett. **3**, 552 (1959).
- ¹⁵ A. Y. Liu, I. I. Mazin, and J. Kortus, Phys. Rev. Lett. **87**, 087005 (2001).
- ¹⁶ H. J. Choi, M. L. Cohen, and S. G. Louie, Phys. Rev. B **73**, 104520 (2006).
- ¹⁷ E. J. Nicol and J. P. Carbotte, Phys. Rev. B **71**, 054501 (2005).
- ¹⁸ M. D. Whitmore, J. P. Carbotte, and E. Schachinger, Phys. Rev. B **29**, 2510 (1984).
- ¹⁹ P. Morel and P. W. Anderson, Phys. Rev. **125**, 1263 (1962).
- ²⁰ A. E. Karakozov and E. G. Maksimov, Sov. Phys. JETP **74**, 401 (1978).
- ²¹ G. D. Gaspari and B. L. Gyorffy, Phys. Rev. Lett. **28**, 801 (1972).
- ²² W. E. Pickett, Phys. Rev. B **25**, 745 (1982).
- ²³ S. Baroni, A. Dal Corso, S. de Gironcoli, P. Giannozzi, C. Cavazzoni, G. Ballabio, S. Scandolo, G. Chiarotti, P. Focher, A. Pasquarello, K. Laasonen, A. Trave, R. Car, N. Marzari, A. Kokalj, <http://www.pwscf.org/>.
- ²⁴ J. J. Hopfield, Phys. Rev. B **186**, 443 (1969).
- ²⁵ J. M. Ziman, *Principle of the Theory of Solids* (Cambridge University Press, Cambridge, 1965), p. 209.
- ²⁶ J. M. An and W. E. Pickett, Phys. Rev. Lett. **86**, 4366 (2001).
- ²⁷ J. E. Han, O. Gunnarsson, and V. H. Crespi, Phys. Rev. Lett. **90**, 167006 (2003).
- ²⁸ C. Falter and M. Selmke, Phys. Rev. B **24**, 586 (1981).
- ²⁹ J. M. An, S. Y. Savrasov, H. Rosner, and W. E. Pickett, Phys. Rev. B **66**, 220502(R) (2002).
- ³⁰ J. K. Dewhurst, S. Sharma, C. Ambrosch-Draxl, and B. Johansson, Phys. Rev. B **68**, 020504(R) (2003).
- ³¹ J. C. Phillips, *Bonds and Bands in Semiconductors* (Academic, New York, 1973).
- ³² H. J. Choi, D. Roundy, H. Sun, M. L. Cohen, and S. G. Louie, Phys. Rev. B **66**, 020513(R) (2002).
- ³³ H. Rosner, A. Kitaigorodsky, and W. E. Pickett, Phys. Rev. Lett. **88**, 127001 (2002).
- ³⁴ E. A. Ekimov, V. A. Sidorov, E. D. Bauer, N. N. Mel'nik, N. J. Curro, J. D. Thompson, and S. M. Stishov *et al.*, Nature (London) **428**, 542 (2004).
- ³⁵ Y. Takano, M. Nagao, T. Takenouchi, H. Umezawa, I. Sakaguchi, M. Tachiki, and H. Kawarada, Diamond Relat. Mater. **14**, 1936 (2005).
- ³⁶ J. E. Lowther, J. Phys.: Condens. Matter **17**, 3221 (2005).
- ³⁷ J. P. Goss and P. R. Briddon, Phys. Rev. B **73**, 085204 (2006).
- ³⁸ Y. Ma, J. S. Tse, T. Cui, D. D. Klug, L. Zhang, Y. Xie, Y. Niu, and G. Zou, Phys. Rev. B **72**, 014306 (2005).
- ³⁹ M. Côté and M. L. Cohen, Phys. Rev. B **55**, 5684 (1997).